Membrane Curvature Change Induced by an Antimicrobial Peptide Detected by ^{31}P Exchange NMR

P. A. B. Marasinghe,[†] J. J. Buffy,[‡] K. Schmidt-Rohr, and M. Hong*

Department of Chemistry, Iowa State University, Ames, Iowa 50011

Received: August 6, 2005; In Final Form: September 20, 2005

The influence of an antimicrobial peptide, protegrin-1 (PG-1), on the curvature and lateral diffusion coefficient (D_L) of phosphocholine bilayers is investigated using one- (1D) and two-dimensional (2D) ^{31}P exchange NMR. The experiments utilize the fact that lipid lateral diffusion over the curved surface of vesicles changes the molecular orientation and thus the ^{31}P chemical shift anisotropy. This reorientation is manifested in 2D spectra as off-diagonal intensities and in 1D stimulated-echo experiments as reduced echo heights. The 2D spectra give information on the reorientation-angle distribution while the decay of the stimulated-echo intensity, which closely tracks the second-order correlation function in our experiments, yields the correlation times of the reorientation. The relationships among the 2D exchange spectra, stimulated-echo intensities, the correlation function, and reorientation-angle distributions are analyzed in detail. In the absence of PG-1, both dilaurylphosphotidylcholine (DLPC) and palmitoyloleoylphosphatidylcholine (POPC) vesicles show biexponential decays of the stimulated-echo intensities to equilibrium values of 0.20−0.25, suggesting that the curvature of the lipid vesicles has a bimodal distribution. The addition of PG-1 to DLPC vesicles increased the decay time constants, indicating that D_L decreases due to peptide binding. In contrast, the addition of PG-1 to POPC vesicles decreased the decay constants by three to fivefold, indicating that the POPC vesicles are fragmented into smaller vesicles. On the basis of the changes in D_L and the decay constants, we estimate that the radius of the POPC vesicles decreases by threefold due to PG-1 binding. Simulations of the 2D exchange spectra yielded quantitative reorientation-angle distributions that are consistent with the bimodal distributions of the vesicle curvature and the effects of the peptide on the two types of lipid bilayers. Thus, ^{31}P exchange NMR provides useful insights into the membrane morphological changes induced by this antimicrobial peptide.

Introduction

Lipid lateral diffusion is a ubiquitous dynamic process in lamellar bilayers. Its rate depends on the viscosity of the membrane and the concentration of obstacles such as membrane proteins. Many experimental and theoretical studies have been conducted to determine the lateral diffusion coefficients of lipids as a function of the membrane composition, barrier concentration, temperature, and hydration.[1−4] However, comparatively few studies have employed lateral diffusion as a probe for the shape and size of lipid vesicles.[5−7] When lateral diffusion occurs on the curved surface of lipid vesicles, it becomes a rotation. Solid-state NMR spectroscopy is particularly adept at detecting molecular reorientations, since nuclear spin frequencies inherently depend on the angle of the molecule-fixed spin interaction tensors with respect to the magnetic field.

The diffusion coefficients, D_L, are related to the radius of curvature, r, and the lateral-diffusion correlation time, τ_{ld}, according to $\tau_{ld} = r^2/6D_L$. Typical lateral-diffusion coefficients of phospholipids in the liquid-crystalline L_α phase are 10^{-7}−10^{-8} cm^2/s.[8,9] For lipid vesicles with a diameter of 1 μm, which are readily produced by freeze-thawing or extrusion, significant reorientations occur on the time scale of 10−100 ms. Rotations on this time scale can be detected using 2D exchange NMR, where an orientation-dependent frequency is measured at two different times, t_1 and t_2, separated by a mixing period t_m. When molecular reorientations occur during t_m, the two frequencies differ. Correlation of the two frequencies ω_1 and ω_2 gives rise to off-diagonal intensities in the 2D spectra. By analyzing the 2D intensity distribution, one can obtain information on the reorientation-angle distributions of motion.[10−12]

One of the most suitable spin interactions for probing lateral-diffusion-induced reorientation of phospholipids is the ^{31}P chemical shift anisotropy (CSA).[13] For liquid-crystalline lipid bilayers, the ^{31}P CSA has a large width of about 45 ppm and uniaxial symmetry, which simplifies the extraction of the reorientation angle. The 100% natural abundance and the relatively high gyromagnetic ratio of the ^{31}P spin further make 2D ^{31}P exchange NMR a sensitive technique.

Recently, a time correlation function formalism[14] was used to determine the correlation time of lateral diffusion from 2D ^{31}P exchange spectra of melittin-bound dipalmitoyl-phosphatidylcholine (DPPC) bilayers.[15] The analysis was based on the fact that the intensity of the 2D exchange spectra, $S(\omega_1, \omega_2; t_m)$, is related to the second-order correlation function $C_2(t_m)$ as

$$C_2(t_m) = \frac{5}{\delta^2} \int\int \omega_1\, \omega_2\, S(\omega_1,\omega_2; t_m)\, d\omega_1\, d\omega_2 \qquad (1)$$

where the frequencies are referenced to the isotropic chemical shift.[14] Integration of a series of 2D spectra measured as a

* To whom correspondence should be addressed. Tel: 515-294-3521. Fax: 515-294-0105. E-mail: mhong@iastate.edu.

[†] Current address: Department of Chemistry, Minnesota State University Moorhead, Moorhead, MN 56563.

[‡] Current address: Department of Chemistry & Biochemistry, University of Minnesota, Minneapolis, MN 55455.

10.1021/jp054396i CCC: $30.25
Published on Web 11/02/2005

function of t_m yields an exponentially decaying curve $C_2(t_m)$ where the decay constant is the diffusion correlation time. While this 2D analysis yields a well-defined correlation time, it has the limitations that the 2D spectral integration is sensitive to finite line widths and other spectral imperfections and that it requires the measurement of a series of many 2D spectra.

A more reliable and efficient way of obtaining information on the reorientation correlation time is the stimulated-echo experiment,[16,17] which is the 1D analogue of the 2D exchange technique. When a fixed $t_1 = \tau$ is used in the 2D exchange experiment, at times $t_2 = t_1 = \tau$, a stimulated echo appears whose intensity decays with increasing mixing time, equivalent to the reduction of the 2D diagonal intensity due to increasing reorientational motion. With a suitably chosen τ, the stimulated-echo intensity can almost equal $C_2(t_m)$, as shown below.

In this work, we combine 2D exchange and 1D stimulated echo ^{31}P NMR to investigate the lateral diffusion of phosphatidylcholine lipids in the absence and presence of a membrane-active antimicrobial peptide, protegrin-1 (PG-1). The goal is to understand whether and how PG-1 binding changes the curvature of lipid vesicles, either by breaking up the vesicles into smaller fragments or by fusing different vesicles into larger liposomes. The change in the vesicle curvature is probed through the lateral-diffusion-induced lipid reorientation on the millisecond time scale. Interest in antimicrobial peptides arises from the rapid and potent antibiotic activity of these molecules against a wide spectrum of microbial organisms.[18,19] PG-1 is a β-hairpin peptide stabilized by two disulfide bonds and is representative of a number of β-sheet antimicrobial peptides.[20] While these peptides are known to exert their antimicrobial activity by disrupting the cell membranes of the target organisms, the molecular mechanism of action is still not well understood. We previously found that PG-1 induces membrane orientational disorder in bilayers of palmitoyloleoylphosphatidylcholine (POPC), whose acyl chains contain 16 and 18 carbons, but not in bilayers of dilaurylphosphatidylcholine (DLPC), which have 12 carbons per acyl chain.[21] In this work, we show by ^{31}P NMR that PG-1 binding slows down the reorientation of DLPC lipids by a factor of 3 but speeds up the reorientation of POPC lipids by a factor of 3 to 5. These indicate that PG-1 binding reduces the radius of POPC vesicles about threefold. In other words, ^{31}P exchange NMR provides direct evidence that PG-1 fragments POPC lipid vesicles.

Theory

Reorientation-Angle Distribution. A 2D exchange spectrum $S(\omega_1, \omega_2; t_m)$ represents the joint probability of finding the nuclear spin with frequency ω_1 at a certain time 0 and with frequency ω_2 at a time t_m later. For interactions with an asymmetry parameter η of 0, such as the ^{31}P chemical shift tensor of liquid-crystalline lipids, the Euler angles Ω describing the relative orientation of the tensor principal-axis system (PAS) with respect to the external magnetic field are simplified to a single angle, the angle between the unique axis of the tensor before and after t_m. Thus, the orientational change of the chemical shift tensor due to motion during the mixing time can also be summarized by a single angle, β, the reorientation angle. Under these conditions, a 2D exchange spectrum is the superposition of basis spectra $S_\beta(\omega_1,\omega_2)$ for different β-angles weighted by the reorientation-angle distribution, $R(\beta; t_m)$

$$S(\omega_1,\omega_2; t_m) = \int_0^{90} d\beta\, R(\beta; t_m)\, S_\beta(\omega_1,\omega_2) \qquad (2)$$

The basis spectra $S_\beta(\omega_1, \omega_2)$ exhibit characteristic elliptical patterns and straight 90° edges.[10,12] For $\beta = 0°$ at $t_m = 0$, the spectrum is purely diagonal. As β increases with t_m, the off-diagonal intensity increases. Simulation of the experimental 2D exchange spectra thus yields $R(\beta; t_m)$.[11] The reorientation-angle distribution provides valuable insights into the geometry of motion, such as the shape of the lipid vesicles. The $R(\beta; t_m)$ function depends parametrically on the mixing time t_m. For isotropic diffusion, where all molecular orientations are equally probable, the $R(\beta; t_m)$ at a long t_m is the surface element $\sin\beta$.

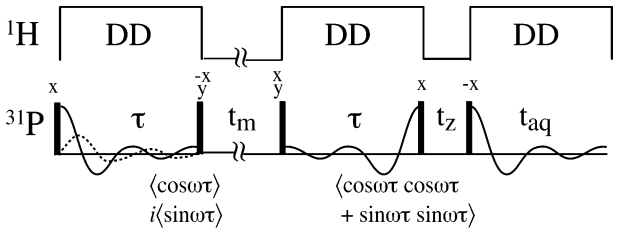

Figure 1. Pulse sequence for the 1D stimulated-echo experiment. Magnetization components are combined using the basic phase cycle indicated to generate a pure stimulated echo. The full echo shown is obtained without frequency change during t_m after two scans have been co-added. The mixing time and the z-filter are interchanged for the control experiment (S_0) to remove T_1 relaxation effects in the normalized exchange signal, S/S_0.

The stimulated-echo experiment is the 1D analogue of the 2D exchange technique, in that the evolution time of the 2D experiment is reduced to a fixed dephasing period τ before t_m (Figure 1). An identical τ delay follows the mixing period to reach the echo maximum. Then a pair of 90° pulses sandwiching a z-filter is applied to select the proper magnetization component and to control for T_1 relaxation effects. The two 90° pulses before and after t_m are phase cycled in synchrony such that a $\cos(\omega_1\tau)\cos(\omega_2\tau)$ term is coadded with a $\sin(\omega_1\tau)\sin(\omega_2\tau)$ term every two scans. This generates a pure stimulated echo, $M_{SE}(\tau,\delta,\eta; t_m)$, after two consecutive scans

$$M_{SE}(\tau,\delta,\eta; t_m) = M_0 \langle \cos(\omega_1\tau)\cos(\omega_2\tau) + \sin(\omega_1\tau)\sin(\omega_2\tau)\rangle$$
$$= M_0 \langle \cos((\omega_1 - \omega_2)\tau)\rangle = \int_{-\delta/2}^{\delta} \cos((\omega_1 - \omega_2)\tau) \times S(\omega_1,\omega_2; t_m)\, d\omega_1\, d\omega_2 \qquad (3)$$

In this equation, M_0 is the full magnetization and δ and η designate the anisotropy parameter and asymmetry parameter, respectively, of the chemical shift tensor. The pointed brackets indicate powder averaging, which is calculated using the 2D spectrum $S(\omega_1,\omega_2; t_m)$ as the probability density of finding the molecules with frequency ω_1 during t_1 and frequency ω_2 after t_m.

When $t_m = 0$, there is no frequency change and $\omega_1 = \omega_2$; then, eq 3 is simplified to

$$M_0 = \int_{-\delta/2}^{\delta} S(\omega_1,\omega_2; t_m)\, d\omega_1\, d\omega_2$$

This means that molecules with different orientations contribute intensities constructively, forming a full echo with a maximal intensity M_0. With increasing t_m, molecular reorientation changes ω_2 from ω_1 and the echo intensity decreases. For symmetric n-site jumps, the stimulated-echo intensity decays exponentially with t_m with a characteristic time constant τ_c

$$M_{SE}\left(\tau \gg \frac{1}{\delta}; t_m\right) = \frac{1}{n} + \left(1 - \frac{1}{n}\right) M_0 e^{-t_m/\tau_c} \qquad (4)$$

It has been shown[22] that the stimulated-echo intensity for a uniaxial interaction ($\eta = 0$) and for a specific reorientation angle

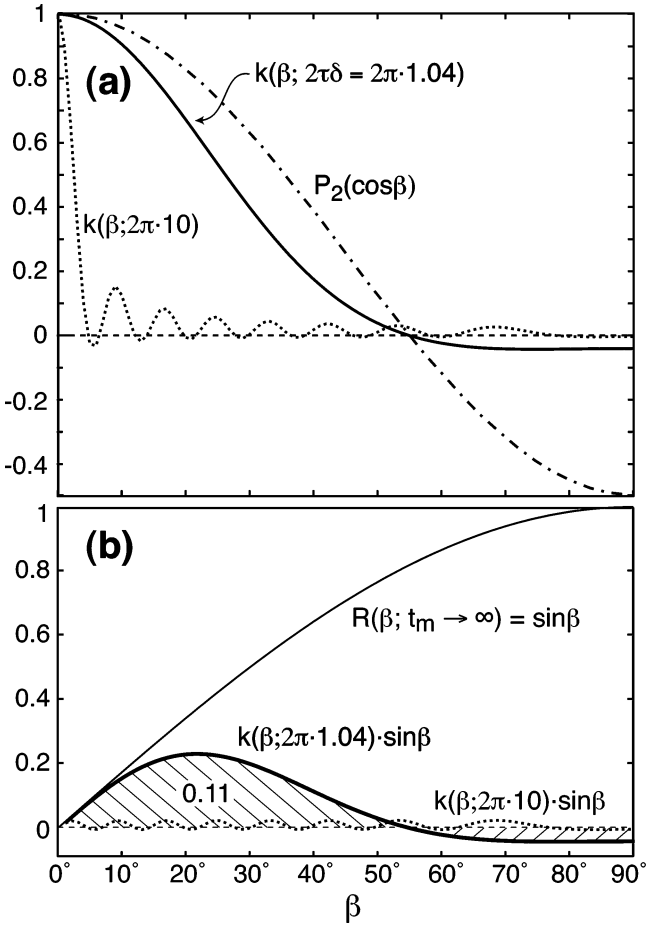

Figure 2. (a) Kernels $k(\beta; 2\tau\delta)$ of the integral of $R(\beta; t_m)$ that determines the stimulated-echo intensity at the given t_m, for $\delta = 5.2$ kHz and $\tau = 0.1$ ms (solid line) and $\tau = 1$ ms (dotted line). As a function of sin β, the curves have the same shape as a spin-pair REDOR curve. The kernel $P_2(\cos\beta)$ of the second-order correlation function (dash−dotted line) is also shown for comparison. (b) Final-state reorientation-angle distribution for isotropic rotational diffusion and its products with the kernels shown in part a. The area under the product curve is the stimulated-echo intensity under these conditions.

β is equivalent to the time signal of a powder sample, $S_{powd}(2\tau\delta_\Delta; \eta_\Delta)$, where the anisotropy of the effective difference tensor is $2\tau\delta_\Delta = 2\tau(^3/_2)\delta \sin\beta = 3\tau\delta \sin\beta$ and the asymmetry parameter of the difference tensor is $\eta_\Delta = 1$. With a distribution $R(\beta; t_m)$ of reorientation angles, the stimulated-echo signal is the weighted sum of these powder signals

$$M_{SE}(\tau,\delta,\eta; t_m) = \int_0^{90} d\beta\, R(\beta; t_m) S_{powd}(3\delta\tau \sin\beta; \eta_\Delta = 1) = \int_0^{90} d\beta\, R(\beta; t_m) k(\beta; 2\tau\delta) \quad (5)$$

Since a static powder line shape for $\eta = 1$ is the same as the Fourier transform of a rotational echo double resonance (REDOR) time signal,[23] $S_{powd}(2\tau\delta_\Delta; \eta_\Delta = 1)$ as a function of $2\tau\delta_\Delta$ is equal to the well-known two-spin REDOR time signal. When S_{powd} is considered as a function of β, this similarity is most obvious at small angles where $\sin\beta \approx \beta$. This is shown in Figure 2a, which plots the integral kernel $k(\beta; 2\tau\delta) = S_{powd}(3\tau\delta \sin\beta; \eta_\Delta = 1)$ as a function of β. The kernel has a peak at $\beta = 0$ that narrows with increasing τ. Only portions of $R(\beta; t_m)$ within this peak contribute significantly to the integral and determine the stimulated-echo intensity. A similar treatment has been given for the $\langle \sin(\omega_1\tau)\sin(\omega_2\tau)\rangle$ stimulated echo in refs 16 and 17.

The kernel $k(\beta; 2\tau\delta)$ can also be calculated from a series of 2D exchange spectra $S_\beta(\omega_1,\omega_2)$, based on eqs 3 and 2

$$M_{SE} = \int\int d\omega_1\, d\omega_2 \cos(\omega_1 - \omega_2)\tau S(\omega_1,\omega_2; t_m) = \int\int d\omega_1\, d\omega_2 \cos(\omega_1 - \omega_2)\tau \int d\beta R(\beta; t_m) S_\beta(\omega_1,\omega_2) = \int d\beta\, R(\beta; t_m) \int\int d\omega_1\, d\omega_2 \cos(\omega_1 - \omega_2)\tau S_\beta(\omega_1,\omega_2) \quad (6)$$

Comparing with eq 5, we find that

$$k(\beta; 2\tau\delta) = \int\int d\omega_1\, d\omega_2 \cos(\omega_1 - \omega_2)\tau S_\beta(\omega_1,\omega_2) \quad (7)$$

Long-Time Behavior of the Stimulated-Echo Intensity. On the basis of eq 5, we can show that for isotropic reorientations, the stimulated-echo intensity does not decay to zero even as t_m approaches infinity, despite the fact that all orientational memory is lost. Consider the product in the integral of eq 5. The first factor $R(\beta; t_m)$ approaches sin β as $t_m \rightarrow \infty$ (Figure 2b). The second factor $k(\beta; 2\tau\delta)$ has a peak at $\beta = 0$, with $k(0) = 1$ (Figure 2a). Since $k(\beta; 2\tau\delta)$ narrows with increasing τ, for small $2\tau\delta$ values, both factors are mostly nonzero and positive, thus the integral over β, that is, the stimulated-echo intensity of eq 5, does not reach zero, as shown by the hatched area under the solid curve in Figure 2b. As τ increases, $k(\beta; 2\tau\delta)$ becomes more restricted to the small β region (dotted line in Figure 2a), where $R(\beta; t_m) = \sin\beta$ is small. Thus, the stimulated-echo intensity, shown as the area under the dotted curve in Figure 2b, approaches zero more closely.

For the liquid-crystalline lipids studied here, the ^{31}P CSA and the stimulated-echo delay time used give $2\tau\delta = 200\ \mu s \times 2\pi \times 32$ ppm $\times$ 162.1 Hz/ppm $= 2.08\pi$. This yields a half width of $f = 27°$ for the kernel $k(\beta)$ (solid line in Figure 2a). Through the use of a step-function approximation to $k(\beta)$, for this width, the integral of the product of sin β with the step function gives $M_{SE} \approx 1 - \cos(f) = 0.11$. This agrees well with the result of the exact calculation using the actual $k(\beta)$. For anisotropic reorientation, the plateau value of the stimulated-echo intensity will be higher, since $R(\beta; t_m \rightarrow \infty)$ is larger at or near $\beta = 0$.

Motional Correlation Times. In a diffusively reorienting system, motions occur with more than one correlation time. Well-defined correlation times of reorientational motion are the time constants $\tau_{c,n}$ of the correlation functions $C_n(t_m)$, which are related to the reorientation-angle distribution as

$$C_n(t_m) = \langle P_n(\cos\beta)\rangle = \int_0^{90} d\beta\, R(\beta; t_m) P_n(\cos\beta) \quad (8)$$

where $P_n(x)$ is the nth Legendre polynomial. For isotropic rotational diffusion, $\tau_{c,n} = n(n+1)\tau_{c,0}$,[24] thus, the correlation times for different n values can differ by orders of magnitude. The correlation time we extract from the 2D exchange experiments is $\tau_{c,2}$, since it is the least sensitive to the fine details of the spectral intensity or noise. We use eq 8 with $n = 2$ to calculate the values of $C_2(t_m)$ for various mixing times, with $R(\beta; t_m)$ distributions that reproduce the measured stimulated-echo intensity according to eq 5 and that give good fits to the 2D exchange spectra. Each 2D spectrum or $R(\beta; t_m)$ gives one point in $C_2(t_m)$. Since $P_2(\cos\beta) = (3\cos^2\beta - 1)/2$ is a slowly varying function, small variations in $R(\beta; t_m)$ do not affect the value of $C_2(t_m)$ significantly. Thus, the two Gaussian functions used below to approximate the true $R(\beta; t_m)$ should be sufficient to obtain a good approximation to $C_2(t_m)$.

It has been pointed out[25] that, for diffusive motions, the decay constant of the stimulated echo is not the correlation time of $C_2(t_m)$. This can be understood by comparing the expressions for $M_{SE}(t_m)$, eq 5, and for $C_2(t_m)$, eq 8. The kernels of the two integrals, $k(\beta; 2\tau\delta)$ and $P_2(\cos\beta)$, are generally not the same. Unless $R(\beta; t_m)$ contains a sharp peak at $\beta = 0$ for all t_m values,

TABLE 1: Stimulated-Echo Time Constants and Weights of DLPC and POPC in the Absence and Presence of PG-1

	double exponential[a]					stretched exponential[b]	
lipid	$\tau_{SE,1}$ (ms)	m_1	$\tau_{SE,2}$ (ms)	m_2	m_0	$\tau_{SE,3}$ (ms)	p
DLPC	1.1 ± 0.2	49%	14 ± 3	25%	25%	2.5 ± 0.3	0.62
DLPC+PG-1	1.9 ± 0.4	38%	52 ± 19	28%	34%	7.9 ± 1.5	0.43
POPC	1.4 ± 0.3	46%	25 ± 7	35%	20%	4.7 ± 0.6	0.52
POPC+PG-1	0.27 ± 0.07	35%	8.0 ± 0.5	22%	42%	1.2 ± 0.2	0.42

[a] The double exponential function is $M_{SE} = m_0 + m_1 e^{-t_m/\tau_{SE,1}} + m_2 e^{-t_m/\tau_{SE,2}}$. [b] The stretched exponential function is $M_{SE} = m_0 + e^{-(t_m/\tau_{SE,3})^p}$.

TABLE 2: Gaussian Widths ($\sigma_{\beta,i}$) and Weights (w_i)[a] of the Reorientation-Angle Distributions of Various Membrane Samples Determined from 2D ^{31}P Exchange Spectra[b]

lipids	t_m	$\sigma_{\beta,1}$	w_1	$\sigma_{\beta,2}$	w_2	$C_2(t_m)$	$M_{SE,calcd}$	$M_{SE,exp}$
DLPC	1 ms	4°	25%	20°	75%	0.77	0.67	0.66
	5 ms	9°	27%	40°	73%	0.44	0.42	0.42
	400 ms	20°	27%	80°	73%	0.19	0.24	0.23
DLPC	1 ms	2°	42%	18°	58%	0.85	0.78	0.78
+ PG-1	5 ms	4°	42%	31°	58%	0.67	0.62	0.62
	400 ms	17°	42%	90°	58%	0.32	0.36	0.34
POPC	1 ms	5°	25%	18°	75%	0.81	0.69	0.70
	5 ms	10°	25%	29°	75%	0.59	0.48	0.50
	50 ms	18°	30%	70°	70%	0.24	0.26	0.28
	300 ms	26°	30%	90°	70%	0.16	0.20	0.21

[a] The Gaussian function is defined in eq 12. [b]The corresponding second-order correlation function values and the calculated and experimental stimulated-echo intensities are also given.

as it does for the jump processes, the time constants of $C_2(t_m)$ and $M_{SE}(t_m)$ need not be the same. However, with our choice of $2\tau\delta$, $k(\beta; 2\tau\delta)$ resembles $P_2(\cos\beta)$ quite closely, see the solid and dash−dotted lines in Figure 2a, so the time constants of the stimulated-echo decays will be close to the true correlation times. This is confirmed by the quantitative calculations below. Moreover, the change in the stimulated-echo decay constant due to the addition of peptides can be determined quantitatively. For an n-times faster motion of the same geometry, the stimulated-echo decay constant will be n-times shorter because the same $R(\beta; t_m)$ will occur at an n-times shorter t_m.

For lipid vesicles, the stimulated-echo intensity can decrease not only due to lateral diffusion over the curved vesicle surface but also due to the overall tumbling of the vesicles in water. The overall correlation time, τ_c, is related to the diffusion correlation time τ_{ld} and the tumbling correlation time τ_{tm} according to

$$\frac{1}{\tau_c} = \frac{1}{\tau_{ld}} + \frac{1}{\tau_{tm}} \tag{9}$$

As mentioned above, τ_{ld} depends on D_L and the vesicle radius r according to

$$\tau_{ld} = \frac{r^2}{6D_L} \tag{10}$$

while the tumbling time τ_{tm} is calculated as

$$\tau_{tm} = \frac{4\pi r^3 \eta_w}{3kT} \tag{11}$$

where η_w is the viscosity of water, k is the Boltzmann constant, and T is the absolute temperature. Using a viscosity of 0.891×10^{-3} kg/(m·s) for water, a radius of 1 μm, and T of 295 K, we find a τ_{tm} of 920 ms. The viscosity of 75% hydrated (w/w) lipid samples used in this study is likely much higher than the viscosity of pure water, thus this estimated τ_{tm} is a lower limit.

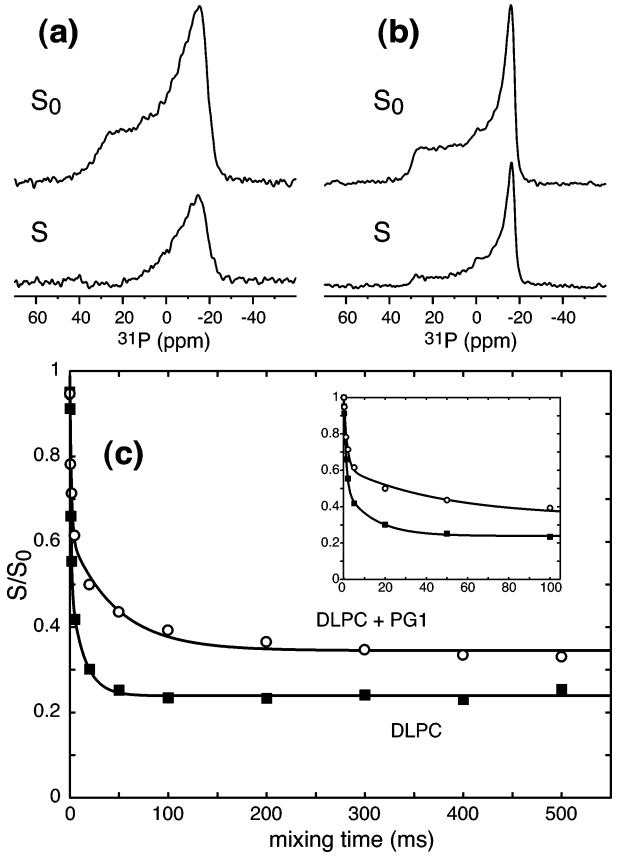

Figure 3. 1D stimulated-echo spectra of DLPC alone (a) and DLPC with PG-1 (b) at a mixing time of 20 ms: S_0, control spectrum; S, exchange spectrum. (c) Normalized stimulated-echo intensities S/S_0 for DLPC (squares) and DLPC/PG-1 (circles) membranes as a function of mixing time. Parameters for the best-fit biexponential decays are listed in Table 1. The inset shows the decay in the initial 100 ms, where a fast component is observed for both samples.

This means that the lateral-diffusion-induced reorientation is faster by 1 to 2 orders of magnitude than vesicle tumbling and τ_c can be approximated as τ_{ld} in eq 9.

Materials and Methods

Sample Preparation. 1,2-dilauryl-*sn*-glycero-3-phosphotidylcholine (DLPC) and 1-palmitoyl-2-oleoyl-*sn*-glycerol-3-phosphatidylcholine (POPC) were purchased from Avanti Polar Lipids (Alabaster, AL) and used without further purification. The acyl chain lengths are 12:0 for DLPC and 16:0 and 18:1 for POPC. The main phase-transition temperatures are −1 °C for DLPC and −2 °C for POPC. PG-1 was synthesized according to a previously published procedure.[26]

Unoriented lipid vesicles were prepared by codissolving appropriate amounts of PG-1 and lipids in TFE and chloroform solutions to achieve a peptide/lipid molar ratio (P/L) of 1:30 or 0. About 25 mg of lipid was dissolved in 2 mL of chloroform, and PG-1 was dissolved in 1 mL of TFE. The lipid and peptide

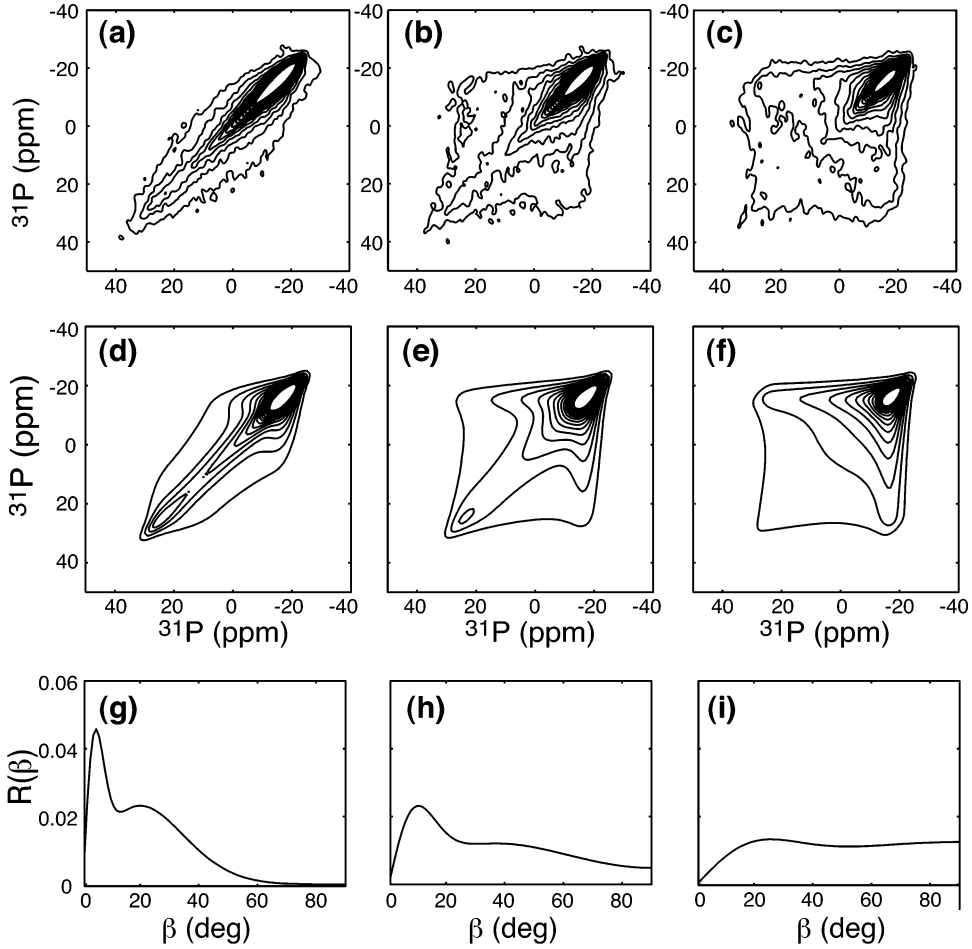

Figure 4. 2D ^{31}P exchange spectra of DLPC bilayers with mixing times of (a) 1 ms, (b) 5 ms, and (c) 400 ms. (d−f) Simulated spectra for a−c. The experimental stimulated-echo intensities are 0.66 (1 ms), 0.42 (5 ms), and 0.23 (400 ms). (g−i) Reorientation-angle distributions $R(\beta; t_m)$ obtained from the best fits.

solutions were mixed and dried under a stream of nitrogen gas, and the resulting film was redissolved in cyclohexane, frozen in liquid nitrogen, and lyophilized. The mixture was then rehydrated with deionized water to 75% (w/w) hydration. The hydrated mixture was vortexed and freeze-thawed five times to obtain a relatively uniform vesicle size of 1 μm.[27,28] The well-hydrated membrane mixtures were center packed into 5-mm diameter glass tubes using a 50-μL microdispenser (Drummond Scientific) and capped with a Teflon plug and Teflon tape.

Solid-State NMR Experiments. NMR experiments were carried out on a Bruker DSX-400 spectrometer (Karlsruhe, Germany) operating at a resonance frequency of 162.12 MHz for ^{31}P (9.4 T). A static double-resonance probe with a horizontal 5-mm diameter radio frequency (rf) coil was used. All experiments were conducted at 295 ± 2 K. Typically, a ^{31}P 90° pulse length of 5 μs, ^{1}H decoupling field strength of 50 kHz, and recycle delays of 2−3 s were used. The ^{31}P chemical shift was referenced externally to phosphoric acid at 0 ppm.

Both the 2D exchange and 1D stimulated-echo experiments were initiated from direct ^{31}P polarization by a 90° pulse. The 2D experiment used the standard three-pulse sequence, 90° − t_1 − 90° − mixing − 90° − detection. The stimulated-echo pulse sequence (Figure 1) includes fixed τ periods before and after the mixing time to encode the ^{31}P CSA and sense the molecular orientation. We used $\tau = 100$ μs in all experiments. At the end of the second τ period, a z-filter was added to correct for T_1 relaxation effects. This involved normalizing the intensity of the exchange experiment (S) to that of a control experiment (S_0) in which the values of t_m and t_z are interchanged. With a short t_z of 10 μs in the first longitudinal period, no reorientation can occur, thus a full stimulated echo results. The sum of t_m and t_z was kept the same between the S and S_0 experiments so that the effects of ^{31}P T_1 relaxation are removed in the normalized intensity, S/S_0. This T_1 correction method is identical to that of the CODEX experiment,[29] which is the magic-angle spinning analogue of the stimulated-echo experiment.

Simulation of 2D Exchange Spectra. The 2D exchange spectra and 1D stimulated-echo intensities were calculated using a Fortran program that also generates the reorientation-angle distribution. The program calculates the frequencies of an axially symmetric chemical shift tensor before and after reorientation. The subspectra for specific β, weighted by $R(\beta; t_m)$, are summed to give the 2D spectra, see eq 2. The stimulated-echo intensity is calculated from the 2D spectrum at the given t_m using eq 3.

Since lipid reorientation is diffusive, $R(\beta; t_m)$ is assumed to consist of Gaussian functions centered at 0° with a width of σ_β

$$R(\beta; t_m) = \sum_i w_i d_i \sin\beta \, e^{-\beta^2/(2\sigma_{\beta,i}^2)} \qquad (12)$$

Here w_i is the weighting factor of the individual Gaussian functions, $\sigma_{\beta,i}$ is the width of each Gaussian, and $d_i = 1/(\sum_{j=0}^{90} \sin\beta_j e^{-\beta_j^2/2\sigma_{\beta,i}^2})$ is the normalization constant for each Gaussian. At short and intermediate mixing times, $\sigma_{\beta,i}$ for diffusive motion increases proportional to $t_m^{1/2}$. Two Gaussian functions ($i = 1$, 2) are necessary to fit the experimental 2D exchange spectra. The actual $R(\beta; t_m)$ function may be more complex, but the two Gaussian fit provides a good approximation, in particular

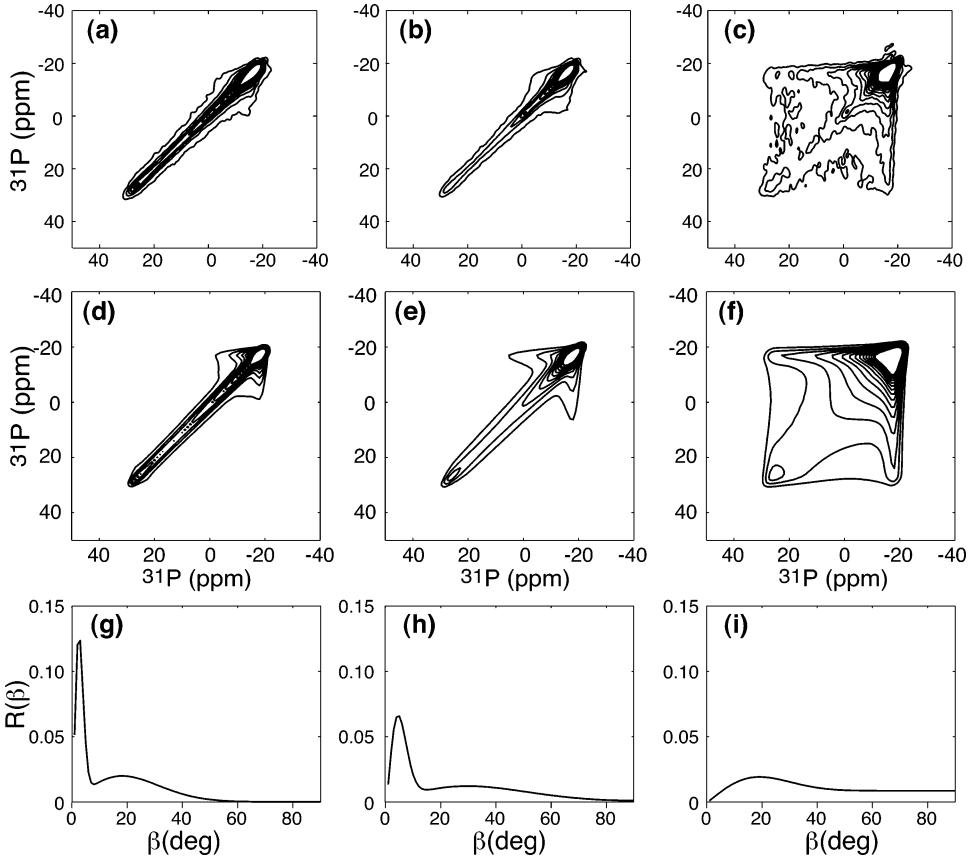

Figure 5. 2D ^{31}P exchange spectra of DLPC/PG-1 membranes after mixing times of (a) 1 ms, (b) 5 ms, and (c) 400 ms. (d−f) Simulated spectra for a−c. The experimental stimulated-echo intensities are 0.78 (1 ms), 0.62 (5 ms), and 0.34 (400 ms). (g−i) Reorientation-angle distributions corresponding to the best-fit simulations.

since it also reproduces the stimulated-echo intensity quantitatively (see Table 2). In the simulations, the angle β is incremented at 3° steps.

The 2D simulations were constrained by four factors: the stimulated-echo intensity for the specific mixing time, the general characteristics of the 2D spectra, the 0° and 90° cross sections of the 2D spectra, and the spectrum along the diagonal. The 2D characteristics optimized were the length of the diagonal ridge, the width perpendicular to the diagonal, and the lowest contour levels. The spectrum along the diagonal was extracted in Matlab. The simulated and experimental spectra are plotted with identical contour levels in all figures shown here.

In simulating the 2D spectra, we found it necessary to use a larger line broadening along the diagonal than perpendicular to the diagonal. The diagonal line broadening is 1−3 ppm to reproduce the experimental features, while the off-diagonal line broadening is typically less than 1 ppm. This indicates that the line width is correlated between the two dimensions, which is most likely a result of B_0 inhomogeneity, including susceptibility effects.

Results

PG-1 Interaction with DLPC Bilayers. To determine whether PG-1 binding changes the radius of curvature of lipid vesicles, we need to know both the correlation time τ_{ld} and the diffusion coefficient D_L (eq 10) in the absence and presence of the peptide. The motional correlation times are extracted from the stimulated-echo decay constants. However, D_L, which may change upon PG-1 binding, is not independently measured in these experiments. Therefore, we use the approach of deducing the *change* in D_L due to peptide binding by using control bilayers that are known to maintain their structural integrity in the presence of PG-1. DLPC is a good bilayer system for this purpose. Our previous oriented-membrane experiments showed that DLPC bilayers maintain their orientational order at high concentrations of PG-1 and the peptide is uniaxially mobile and thus likely monomeric in this bilayer.[26] These indicate that no structural and phase changes occur to DLPC bilayers upon PG-1 binding. Thus, it is a reasonable approximation that the DLPC vesicle size is unaffected by peptide binding. By comparing the reorientational correlation times of DLPC lipids in the absence and presence of PG-1, we can then determine whether the diffusion coefficient D_L is changed by PG-1 binding.

Figure 3 shows the stimulated-echo decay curves as a function of t_m for DLPC in the absence (squares) and presence (circles) of PG-1. Two common features are observed. First, both curves decay to a nonvanishing equilibrium value. Second, neither curve follows a single-exponential decay but must be fit with either a double exponential with a constant offset, $m_0 + m_1 e^{-t_m/\tau_{SE,1}} + m_2 e^{-t_m/\tau_{SE,2}}$, or a stretched exponential function, $m_0 + e^{-(t_m/\tau_{SE,3})^p}$, where $p < 1$. For DLPC bilayers, the double-exponential fit gave a fast decay constant of 1.1 ms and a slow constant of 14 ms (Table 1). The stretched exponential fit yielded a time constant of 2.5 ms and a stretching exponent p of 0.62. Since pure DLPC bilayers, as a one-component system, cannot have any dynamical heterogeneity, the multiexponential nature of the decay suggests that the lipid vesicles have more than one radius of curvature. In principle, this distribution may result from a nonspherical shape of the vesicle such as ellipsoids or that the vesicles are multilamellar rather than unilamellar. Since the equilibrium value of 0.25 is significantly larger than the value (0.11) predicted for isotropic diffusion under our experimental conditions (Figure 2b), the nonspherical shape of the

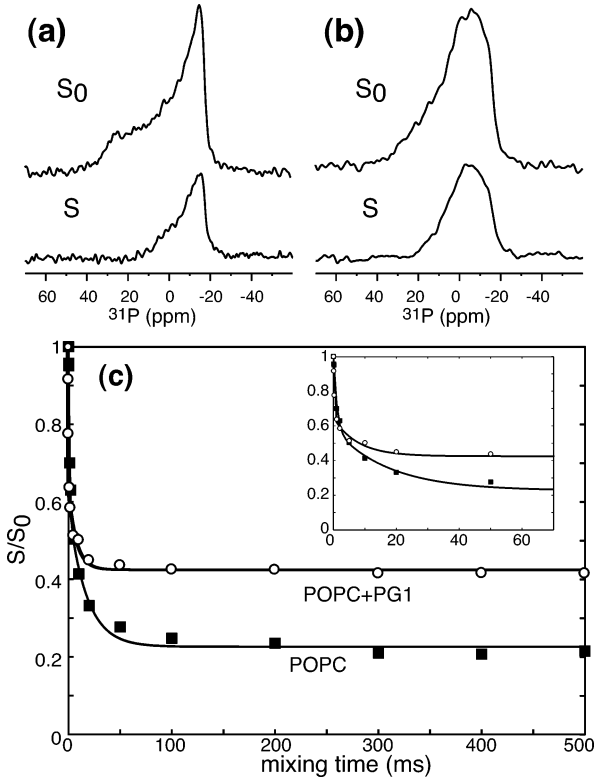

Figure 6. 1D stimulated-echo spectra of POPC alone (a) and POPC with PG-1 (b) at a mixing time of 20 ms: S_0, control spectrum; S, exchange spectrum. (c) Normalized stimulated-echo decays S/S_0 for POPC membranes in the absence (squares) and presence of PG-1 (circles) as a function of mixing time. Inset shows the decays in the initial 70 ms. Best-fit biexponential decays are shown. The fit parameters are listed in Table 1.

vesicles is a more likely reason for the observed multiexponentiality of the decay. In other words, regions of the vesicle with large radii of curvature contribute to slower molecular reorientations or larger time constants.

The addition of PG-1 to DLPC lipids slowed the reorientation, increasing the time constants by about threefold (Table 1). In the double-exponential fit, the long time constant increased from 14 to 52 ms. In the stretched exponential fit, $\tau_{SE,3}$ increased from 2.5 to 7.9 ms. Since previous measurements[21,26] indicated that the structural integrity of DLPC bilayers is well maintained in the presence of PG-1, the increased time constants strongly suggest that the diffusion coefficient decreased due to PG-1 binding; this is consistent with the obstructed diffusion of the lipids in the presence of the peptide.[2] In addition, the equilibrium value increased to ~0.34, suggesting that the shapes of the vesicles may have become more elongated upon peptide binding.

Figure 4 shows the 2D exchange spectra of pure DLPC lipids after mixing times of 1, 5, and 400 ms. As the mixing time increases, the off-diagonal intensity increases as expected, while the stimulated-echo intensity decreases. The stimulated-echo intensities for the three mixing times are 0.66, 0.42, and 0.23 (Table 2). Thus, even at the shortest mixing time of 1 ms, about one-third of the total intensity is off the diagonal. This illustrates the advantage of the stimulated-echo experiment in highlighting motional features that are not readily detectable in the 2D spectra. The simulation of the 2D exchange spectra can be much less accurate without the quantitative value of the relative intensity of the diagonal and off-diagonal intensities given by the stimulated echo.

Consistent with the biexponentiality of the 1D data, the 2D spectral fitting requires at least two Gaussian functions with different widths σ_β (Table 2). The small-angle component contributes intensities mainly along the diagonal, while the large-angle component preferentially contributes off-diagonal intensities. The reorientation-angle distributions $R(\beta; t_m)$ corresponding to the best-fit 2D simulations are shown in the bottom row of Figure 4. The increasing percentage of large-angle reorientations at a long mixing time is evident.

Figure 5 shows the 2D exchange spectra of DLPC bilayers after PG-1 binding. It can be seen that peptide binding increased the diagonal intensities and decreased the off-diagonal intensities

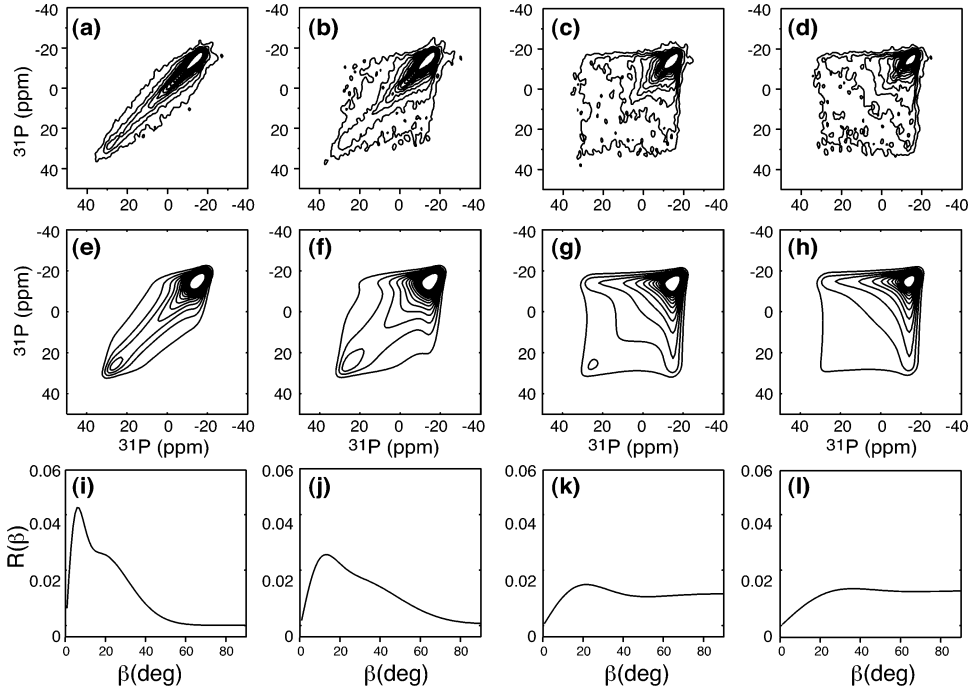

Figure 7. 2D ^{31}P exchange spectra of POPC bilayers with mixing times of (a) 1 ms, (b) 5 ms, (c) 50 ms, and (d) 300 ms. The experimental stimulated-echo intensities are 0.70 (1 ms), 0.50 (5 ms), 0.28 (50 ms), and 0.21 (300 ms). (e−h) Best-fit simulations. (i−l) Reorientation-angle distributions extracted from the best-fit spectra.

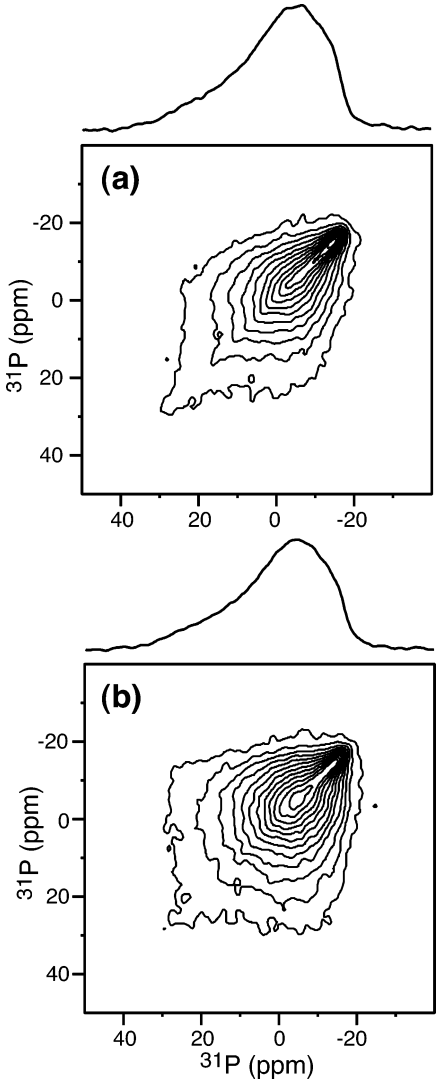

Figure 8. 2D ^{31}P exchange spectra of POPC/PG-1 membranes after mixing times of (a) 1 ms and (b) 10 ms. The experimental stimulated-echo intensities are 0.64 (1 ms) and 0.51 (10 ms).

compared to the pure DLPC membrane. This is consistent with the higher stimulated-echo intensities for the peptide-bound DLPC membrane. Correspondingly, the fraction of small-angle reorientations in the simulations increased in the peptide−lipid mixture. For example, the $R(\beta; t_m)$ function for the 1 ms DLPC/PG-1 spectrum consists of 42% of a Gaussian with a width of 2° and 58% of a Gaussian with a width of 18°. In comparison, the 1 ms DLPC spectrum is fit with 25% of a 4° Gaussian width and 75% of a 20° Gaussian width (Table 2), indicating that lipid lateral diffusion is partially obstructed by PG-1, giving rise to a smaller D_L. Table 2 also lists the $C_2(t_m)$ values for each simulated 2D spectrum. As predicted above, for our choice of $2\delta\tau$, $C_2(t_m)$ is quite similar to the normalized stimulated-echo intensity. Thus, the decay constants from $M_{SE}(t_m)$ will be close to the true correlation times of $C_2(t_m)$. As expected, the addition of the peptide to the DLPC bilayer changed the C_2 values in the same direction as the stimulated-echo intensities. Thus, although we do not extract the true correlation time $\tau_{c,2}$ due to the small number of the 2D spectra collected, the change in the decay constants of the stimulated-echo intensities correctly reflects the change in the true $\tau_{c,2}$ due to peptide binding.

PG-1 Interaction with POPC Lipids. The interaction of PG-1 with POPC lipids contrasts dramatically with its effect on DLPC lipids. Figure 6 shows the stimulated-echo curves of POPC lipids with and without PG-1. While the general features of biexponentiality and finite plateau persist, the addition of PG-1 decreased rather than increased the motional correlation times. Double-exponential fits yielded a fast-decaying component of 1.4 ms for POPC and of 0.27 ms for the POPC−peptide mixture. Similarly, the correlation time of the slow-decaying component decreased from 25 to 8 ms upon peptide binding. The approximate fourfold reduction in the time constants is also seen in the stretched exponential fit, which yielded an average τ_c of 4.7 ms without PG-1 but 1.2 ms with PG-1.

Figure 7 shows the 2D exchange spectra of pure POPC lipids after mixing times of 1, 5, 50, and 300 ms. It is reassuring to observe that the 2D intensity distributions are very similar to those of DLPC (Figure 4). The decay constants extracted from the 1D stimulated-echo decays are also within a factor of 2 of each other. Thus, the lateral-diffusion constants of the two lipids are similar. This is not surprising, since the gel-to-L_α phase-transition temperatures, which determine the fluidity of the lipids, are nearly identical for the two lipids (−1 °C for DLPC and −2 °C for POPC).

The similarity of the POPC and DLPC exchange behavior accentuates the contrast when PG-1 binds to the membranes. Figure 8 shows the 2D exchange spectra of the POPC/PG-1 mixture after mixing times of 1 and 10 ms. Substantial exchange intensities are detected even at 1 ms. Moreover, the ^{31}P line shape, shown as the 2D projection, is partially averaged, indicating the presence of sub-millisecond time scale motions that change the ^{31}P CSA interaction. Thus, the intensity of the control spectrum S_0 already has significant decay, which makes S/S_0 in Figure 6 appear artificially high. Due to the distortion of the ^{31}P CSA powder spectrum, we did not simulate the 2D exchange spectra of the POPC/PG-1 membrane. However, we can estimate the change in the vesicle radius from the measured stimulated-echo decay constants. Using the assumption that the longer time constants in the double-exponential fit correspond to flatter regions of the nonspherical vesicles, and using the result that adding PG-1 reduces the lateral diffusion coefficient D_L by a factor of 3, then a three to fivefold reduction of τ_{ld} indicates that the vesicle radius is reduced by about a factor of 3 due to PG-1 binding.

Discussion

The determination of lipid vesicle sizes from lateral diffusion requires the knowledge of both the diffusion correlation time τ_{ld} and the diffusion constant D_L. Since we do not independently measure D_L, which in principle can be done by using spherical supports of defined sizes,[30] reasonable assumptions have to be made to deduce the vesicle radius. We choose DLPC lipids as a control membrane because it maintains the structural integrity upon PG-1 binding. This is seen from a number of spectroscopic observations, including the ^{31}P powder line shape, which is unperturbed by PG-1, the ^{31}P spectrum of oriented membranes, which is well ordered in the presence of PG-1, and the uniaxial rotation of PG-1 around the DLPC bilayer normal.[26] These indicate that PG-1 is incorporated into the DLPC bilayers similar to lipids. With this assumption, the slower lipid reorientation can only result from the reduction in the diffusion coefficient D_L. This reduction was observed before for other membrane peptides such as melittin[15] and can be understood as the physical obstruction by membrane additives. Various models such as the achaepelogo model have been proposed to explain this obstructed diffusion.[2]

The observation that POPC lipids in the absence of PG-1 have nearly identical 2D exchange spectra and similar stimulated-

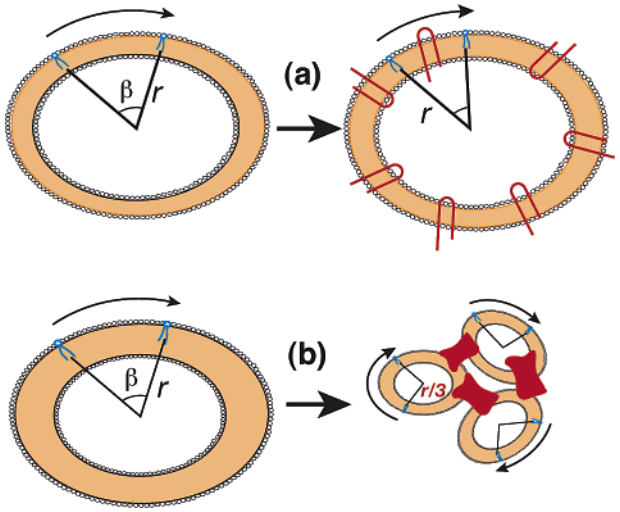

Figure 9. Two modes of PG-1 interaction with phosphocholine lipids. (a) With DLPC lipids, PG-1 hinders the lateral diffusion, reducing D_L by a factor of 3. The vesicle structure remains mostly intact, and the peptide (red) is likely monomeric. (b) With POPC lipids, PG-1 not only reduces D_L but also breaks the vesicles into smaller pieces. The radius is about three times smaller. The peptide is aggregated in this membrane.

echo decay constants as DLPC lipids is expected for lipids with similar liquid-crystalline fluidity and vesicle sizes. Thus, if PG-1 binding does not affect the structural integrity of the POPC vesicles, one would expect the reduced D_L to similarly slow the exchange rate. However, the opposite was observed: the POPC/PG-1 mixture shows a three to fivefold decrease in the stimulated-echo time constant. This can only result from a reduced radius of the vesicles. Using eq 8, we estimate that the vesicle radius is approximately three times smaller as a result of PG-1 binding. This is consistent with the epifluorescence microscopy result of DPPC monolayers in the absence and presence of PG-1, which showed a significant increase of disordered domains upon peptide binding.[31]

Figure 9 summarizes our current understanding of the different effects of PG-1 on DLPC and POPC bilayers. PG-1 maintains the structural integrity of the DLPC bilayer and only reduces the lateral diffusion coefficient. The peptide is likely monomeric in the bilayer. In comparison, PG-1 fragments the POPC vesicles, reducing the vesicle radius by about a factor of 3. The peptide is inserted and aggregated in this membrane.[32] The fact that both POPC and DPPC membranes are fragmented and disordered by PG-1 while the membranes of the short-chain lipid DLPC are not supports the notion that PG-1's membrane-disruptive ability depends on the hydrophobic mismatch between the peptide and the bilayer thickness. This hydrophobic mismatch effect was also manifested in the mobility of PG-1, which was inhibited in the thicker POPC bilayers but present in the thinner DLPC bilayers.[21]

The 1D stimulated-echo experiment is useful for both extracting motional correlation times and providing quantitative constraints to the simulation of the 2D exchange spectra. For systems comprising multiple chemically inequivalent sites, the stimulated-echo experiment can be conducted under MAS, which is the CODEX experiment.[29]

Acknowledgment. We thank E.M. Johnson for assistance in this work. M.H. acknowledges the Alfred P. Sloan Foundation (Grant BR-4151) for a research fellowship. This work is supported by NIH Grant GM-066976.

References and Notes

(1) Vaz, W. L. C.; Goodsaid-Zalduondo, F.; Jacobson, K. *FEBS Lett.* **1984**, *174*, 199.
(2) Saxton, M. J. *Biophys. J.* **1987**, *52*, 989.
(3) Eisinger, J.; Flores, J.; Petersen, W. P. *Biophys. J.* **1986**, *49*, 987.
(4) Lindblom, G.; Oradd, G.; Rilfors, L.; Morein, S. *Biochemistry* **2002**, *41*, 11512.
(5) Auger, M.; Smith, I. C.; Jarrell, H. C. *Biophys. J.* **1991**, *59*, 31.
(6) Macquaire, F.; Bloom, M. *Phys. Rev. E* **1995**, *51*, 4735.
(7) Dolainsky, C.; Unger, M.; Bloom, M.; Bayerl, T. M. *Phys. Rev. E* **1995**, *51*, 4743.
(8) Gennis, R. B. *Biomembranes: Molecular Structure and Function*; Springer: New York, 1989.
(9) Lindblom, G.; Oradd, G. Liquid-crystalline samples: diffusion. In *Encyclopedia of Nuclear Magnetic Resonance*; John Wiley: Chichester, U.K., 1996; p 2760.
(10) Schmidt, C.; Wefing, S.; Blumich, B.; Spiess, H. W. *Chem. Phys. Lett.* **1986**, *130*, 84.
(11) Wefing, S.; Spiess, H. W. *J. Chem. Phys.* **1988**, *89*, 1219.
(12) Schmidt-Rohr, K.; Spiess, H. W. *Multidimensional Solid-State NMR and Polymers*, 1st ed.; Academic Press: San Diego, CA, 1994.
(13) Fenske, D. B.; Jarrell, H. C. *Biophys. J.* **1991**, *59*, 55.
(14) Zemke, K.; Schmidt-Rohr, K.; Spiess, H. W. *Acta Polym.* **1994**, *45*, 148.
(15) Picard, F.; Paquet, M.-J.; Dufourc, E. J.; Auger, M. *Biophys. J.* **1998**, *74*, 857.
(16) Roessler, E. *Chem. Phys. Lett.* **1986**, *128*, 330.
(17) Fujara, F.; Wefing, S.; Kuhs, W. F. *J. Chem. Phys.* **1988**, *88*, 6801.
(18) Epand, R. M.; Vogel, H. J. *Biochim. Biophys. Acta* **1999**, *1462*, 11.
(19) Hancock, R. E.; Scott, M. G. *Proc. Natl. Acad. Sci. U.S.A.* **2000**, *97*, 8856.
(20) Bellm, L.; Lehrer, R. I.; Ganz, T. *Expert Opin. Invest. Drugs* **2000**, *9*, 1731.
(21) Buffy, J. J.; Waring, A. J.; Lehrer, R. I.; Hong, M. *Biochemistry* **2003**, *42*, 13725.
(22) deAzevedo, E. R.; Bonagamba, T. J.; Hu, W.; Schmidt-Rohr, K. *J. Chem. Phys.* **2000**, *112*, 8988.
(23) Gullion, T.; Schaefer, J. *J. Magn. Reson.* **1989**, *81*, 196.
(24) Debye, P. *Polar Molecules*; Dover: New York, 1929.
(25) Geil, B.; Fujara, F.; Silescu, H. *J. Magn. Reson.* **1998**, *130*, 18.
(26) Yamaguchi, S.; Waring, A.; Hong, T.; Lehrer, R.; Hong, M. *Biochemistry* **2002**, *41*, 9852.
(27) Traikia, M.; Warschawski, D. E.; Recouvreur, M.; Cartaud, J.; Devaux, P. E. *Eur. Biophys. J.* **2000**, *29*, 184.
(28) MacDonald, R. C.; Jones, E. D.; Qiu, R. *Biochim. Biophys. Acta* **1994**, *1191*, 362.
(29) deAzevedo, E. R.; Bonagamba, T. J.; Hu, W.; Schmidt-Rohr, K. *J. Am. Chem. Soc.* **1999**, *121*, 8411.
(30) Kochy, T.; Bayerl, T. M. *Phys. Rev. E* **1993**, *47*, 2109.
(31) Gidalevitz, D.; Ishitsuka, Y.; Muresan, A. S.; Konovalov, O.; Waring, A. J.; Lehrer, R. I.; Lee, K. Y. *Proc. Natl. Acad. Sci. U.S.A.* **2003**, *100*, 6302.
(32) Buffy, J. J.; Waring, A. J.; Hong, M. *J. Am. Chem. Soc.* **2005**, *127*, 4477.